



ELSEVIER

Chemical Physics 258 (2000) 181–186

Chemical  
Physics

www.elsevier.nl/locate/chemphys

## Solvation structures in three dimensions

Igor M. Svishchev<sup>a,\*</sup>, Alexander Yu. Zassetsky<sup>a,1</sup>, Peter G. Kusalik<sup>b</sup>

<sup>a</sup> Department of Chemistry, Trent University, Peterborough, Ont., Canada K9J 7B8

<sup>b</sup> Department of Chemistry, Dalhousie University, Halifax, NS, Canada B3H 4J3

Received 12 December 1999

### Abstract

Extensive efforts are currently devoted to the development of experimental and computer simulation methods which enable one to unambiguously elucidate the three-dimensional coordination structures in disordered systems, such as liquids and amorphous solids. The purpose of this paper is to present a simulation technique to study the spatial structures in molecular liquids. The illustrations include the local structures in liquid water at different temperatures and densities and the hydration structures induced by dissolved oxygen molecules in water. © 2000 Published by Elsevier Science B.V. All rights reserved.

### 1. Introduction

The aim of this paper is to guide the reader through a novel simulation technique which may be used to gain an understanding of the three-dimensional (3D) coordination structures in molecular liquids. Our primary focus will be on the microstructure in liquid water, specifically, on its variations with temperature and density and in the presence of dissolved oxygen.

Knowledge of the local coordination of atoms or molecules in liquids and solids is an essential prerequisite to a detailed understanding of their physical and chemical properties. In crystals, where atoms (or groups of atoms) are arranged in

a periodic pattern, the microscopic structure is associated with the 'unit cell' containing relatively few particles which infinitely repeats itself in three dimensions. Particles are permanently fixed in a Cartesian space, or, in other words, in a laboratory frame. The determination of the crystal structure by the diffraction methods and its subsequent modeling is made straightforward by the presence of this permanent long-range order.

In liquids (or amorphous solids), there is no long-range periodicity in the particles positions in a laboratory fixed frame. For this reason, the microscopic structure in a disordered system is usually associated with its average local structure. The local structure is specified by the average (most probable) positions of particles in the local frame of an arbitrary origin atom (molecule). Most of our microscopic information about these short-range structures comes from the analysis of the atom–atom radial distribution functions (RDFs),  $g(r)$ . The RDF characterizes the average density of particles at distance  $r$  from the center of an

\* Corresponding author.

E-mail address: isvishchev@trentu.ca (I.M. Svishchev).

<sup>1</sup> On leave from Kurnakov Institute of General and Inorganic Chemistry, Russian Academy of Sciences, 117907 Moscow, Russia.

arbitrary central atom. The radial distribution function is related by the Fourier transform to the structure factor,  $S(q)$ , where

$$S(q) = 4\pi\rho \int_0^\infty r^2(g(r) - 1) \frac{\sin(qr)}{qr} dr, \quad (1)$$

in which  $\rho$  is the number density of particles in a liquid. In this equation,  $\hbar q$  corresponds to the momentum transfer in a reciprocal space which can be determined experimentally, for example, from the measurements of neutron scattering cross-sections [1]. Historically, computer simulation studies have also relied almost exclusively upon the RDFs in order to depict liquid structures [2].

For molecular systems, the total RDF can be split into individual atom–atom RDFs (the same procedure applies to the total structure factor); for water, they are  $g_{OO}(r)$ ,  $g_{OH}(r)$  and  $g_{HH}(r)$ . By changing the isotopes in a neutron scattering experiment, it appears possible to determine these partial RDFs separately [3,4]. It is important to emphasize that any partial RDF, no matter how detailed it may appear, is the one-dimensional representation of a 3D structure (and as such is spatially averaged) and therefore carries a limited amount of structural information. In many mo-

lecular liquids, particles interact through strongly anisotropic potentials. The local arrangements of neighboring particles in these liquids are non-spherical which limits the utility of a simple radial analysis of molecular coordination. The liquid state structure in water is a particularly instructive example.

## 2. Spatial structure in liquid water

Pennycuik [5], and Bernal and Fowler [6] were the first to realize that the short-range order in water is consistent with the tetrahedral packing pattern in the distribution of oxygen atoms. Later, in their classical experimental study of the X-ray diffraction from liquid water, Morgan and Warren [7] suggested that the first coordination shell in water contains both the tetrahedrally coordinated molecules at approximately 2.8 Å and some additional more distant neighbors, in order to explain the elevated level of molecular pair density at separations corresponding to the first minimum in the  $g_{OO}(r)$  around 3.5 Å. Fig. 1 displays  $g_{OO}(r)$  for liquid water at 298 K. The experimental curve [3] is shown together with the simulation results for the polarizable point charge (PPC) [8] and the TIP4P

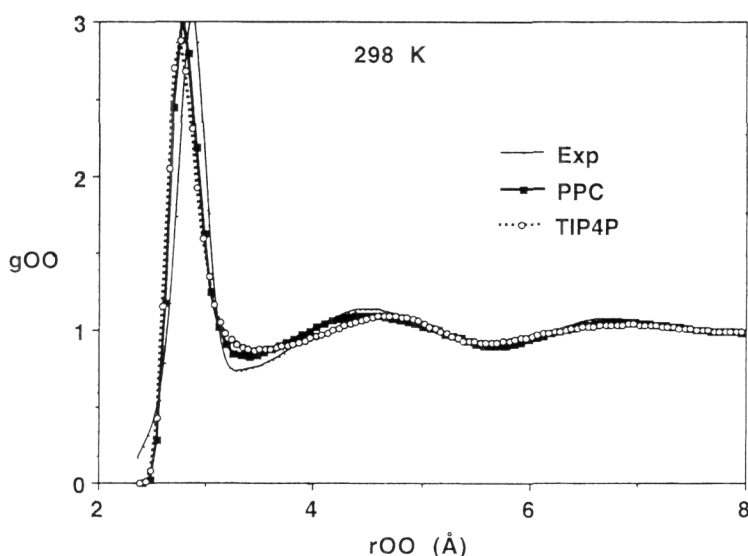


Fig. 1. The radial distribution function of oxygen atoms in liquid water at 298 K. The continuous thin line represents the experimental data [3]. The squares and circles are the simulation results for the PPC and TIP4P models of water, respectively.

[9] models of water. This idea has been developed in detail by Samoilov [10] and Narten et al. [11] into the ‘interstitial’ model for water structure. The ‘interstitial’ model described liquid water as an equilibrium mixture of two fractions, a fraction with the structure of a 3D hydrogen (H) bonded network similar to that of the ice  $I_h$  and a fraction of interstitial molecules occupying the cavities in the ice-like framework (in ice  $I_h$ , each molecule in the lattice is 3.47 Å from six cavity centers).

Another typical assumption about liquid water structure originates from Pople and his concept of H-bond flexibility [12]. Much later, Rice et al. [13] have advanced the original Pople’s model into what has now become known as the continuous random network model.

Since the pioneering works of Rahman and Stillinger [14,15], computer models of water have been extensively examined to elucidate its structure and properties. It is interesting to note that Stillinger and Rahman have attempted to resolve the  $g_{OO}(r)$  into three direction-dependent components which were generated by the faces of a regular icosahedron, in order to achieve a more detailed description of the local orientational order in computer simulated water [14]. By examining their oxygen–oxygen RDF, they have found no evidence for the partitioning of water molecules into two classes.

Obviously, much clarity and detail in liquid structure studies can be achieved by elucidating the full orientation dependent pair-distribution function,  $g(r, \Theta_1, \Theta_2)$ , where  $\Theta$  defines the orientation of a molecule. The full molecule pair-distribution function can be written as an expansion in spherical harmonics and is related (nonuniquely) to the experimentally determined partial atom–atom RDFs [4]. Unfortunately, explicit evaluation and analysis of the full pair-distribution function for water molecules, the function of nine variables (six of them being independent), is a formidable task.

A straightforward and useful method of contracting the full pair-distribution function  $g(r, \Theta_1, \Theta_2)$  has been implemented in the studies of liquid water and other molecular liquids [16–19]. For instance, if one fixes  $H_2O$  molecule 1 at the origin (i.e. sets  $\Theta_1 = 0$ ) and performs averaging

over the orientations of the second  $H_2O$  molecule, then the average spatial positions of atoms can be characterized by the pair-distribution functions  $g_{OO}(r, \Omega)$  and  $g_{OH}(r, \Omega)$ , where  $\Omega = (\theta, \phi)$  represents the angular coordinates of the separation vector in which  $\theta$  denotes the angle between the dipole axis of the central water molecule 1 and the atom–atom separation vector, and  $\phi$  is the angle away from the plane of this central molecule. These contracted pair-distribution functions, known as the spatial distribution functions (SDFs), span both the radial and angular coordinates of the interatomic separation vector and hence are sufficient to characterize the local 3D packing of molecules [16]. The SDF explicitly specifies where, in the space defined by the local frame of the central molecule, are we likely to find a neighboring particle.

Practically, the SDF can be routinely obtained in a simulation at only a modest expense of computer resources. More important is that the SDF can be visualized as the 3D map of the local density making a direct validation of the experimental pair-density maps possible which are now beginning to emerge from neutron scattering data [4,20,21].

The spatial distribution functions of oxygen atoms,  $g_{OO}(r, \Omega)$ , in ambient, 298 K, and high-temperature, 473 K, liquid water are displayed in Fig. 2(a) and (b). The simulation results for the PPC model of water are shown. The SDFs in Fig. 2 are visualized with the aid of the equiprobability surfaces, specifically, at  $g_{OO}(r, \Omega) = 1.6$ . These surfaces confine the spatial domains where the probability density is higher inside than outside. The surfaces in Fig. 2 reflect the oxygen atom of density 1.6 times that of the bulk.

The two distinct caps (marked as 1) in Fig. 2(a) centered directly over the hydrogens of the central molecule at about 2.7 Å from its oxygen atom are due to its two nearest H-bond-accepting neighbors, the single cupped feature (also marked as 1) below the central molecule is due to its two nearest H-bond-donating neighbors, and the two more distant features (which appear confined to the upper hemisphere in the local frame) represent the additional nontetrahedral coordination (marked as A). It is these local interstitial maxima

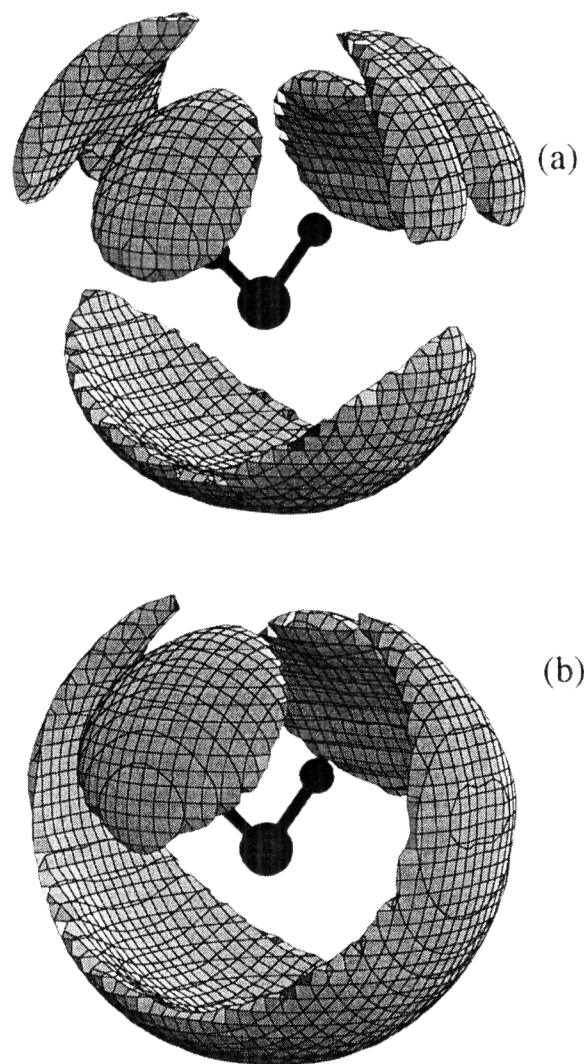


Fig. 2. The effect of temperature on the spatial structure in liquid water. The spatial distributions of oxygen atoms in (a) ambient and (b) high-temperature liquid are displayed. The simulation results for the PPC model of water at density  $1.0 \text{ g/cm}^3$  are shown. I and A identify, respectively, the first H-bond neighbors and the interstitial coordination.

A that are lost in the orientation averaged RDF  $g_{\text{OO}}(r)$ , being responsible for the elevated pair density around its first minimum at about  $3.5 \text{ \AA}$  (Fig. 1).

Remarkably similar density distribution around water molecule in a liquid has been obtained by Soper from experimental data [4]. His approach

uses a maximum entropy constraint to estimate the full molecular pair-distribution function that is consistent with the atom–atom RDFs obtained from neutron scattering.

Fig. 2(b) clearly illustrates that as temperature increases less local neighbors are found above the  $g_{\text{OO}}(r, \Omega = 1.6)$  threshold, and the average structure appears less pronounced. In high-temperature liquid, the nearest neighbors which donate hydrogen atoms in H bonds with the central molecule tend to align along the dipole axis of the central particle. The local peaks in the  $g_{\text{OO}}(r, \Omega)$  due to the interstitial coordination (peaks A) undergo significant broadening with temperature and merge with the nearest H-donor peaks, as can be seen in Fig. 2(b).

Our next focus will be on the local microstructure in high-density low-temperature liquid water. Fig. 3(a) and (b) displays the spatial distribution of oxygen atoms in  $263 \text{ K}$  liquid PPC water at densities of  $1.0$  and  $1.15 \text{ g/cm}^3$ . This figure portrays dramatic changes in the local coordination very different from those caused by temperature increase. In high-density liquid, the interstitial coordination does not appear to merge (coalesce) with the nearest H-bond coordination. It rather forms a distinct hydration shell that interpenetrates the first H-bond neighbor shell as can be clearly seen in Fig. 3(b). A similar bonding pattern (two interpenetrating networks) is present in high-density crystalline ices [22]. Presumably, similar topological changes in the local 3D coordination may also occur when the metastable glassy forms of water undergo densification under applied pressure [23].

### 3. Effect of dissolved oxygen

We now turn our attention to the microstructure induced by the dissolved oxygen molecules. Dissolved oxygen in water is an important species responsible for the oxidation of most organic and inorganic matter in our environment. Yet, virtually no direct microscopic information about its hydration structure exists. Upon freezing, water–oxygen mixtures (under pressure) form a clathrate

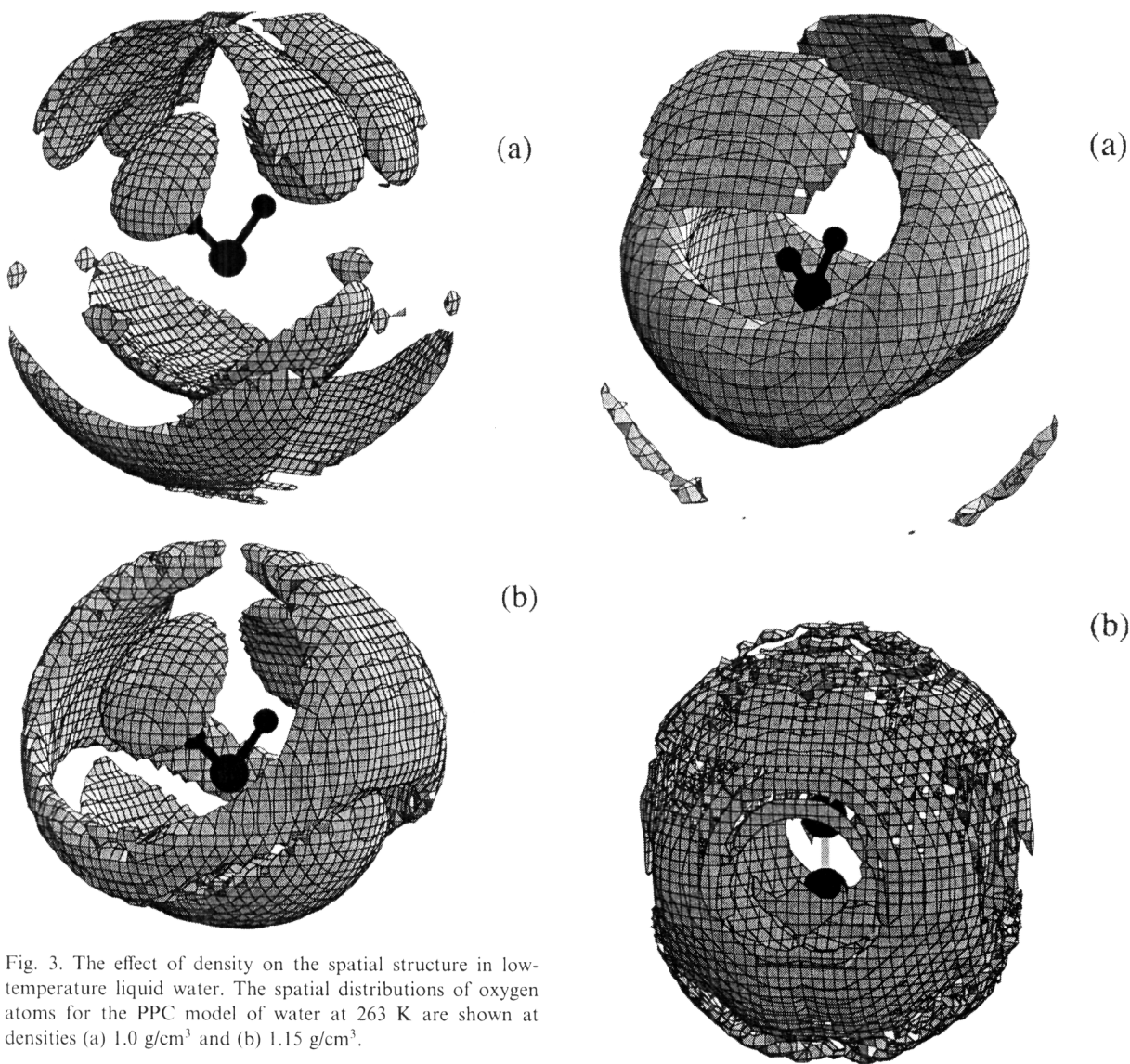


Fig. 3. The effect of density on the spatial structure in low-temperature liquid water. The spatial distributions of oxygen atoms for the PPC model of water at 263 K are shown at densities (a) 1.0 g/cm<sup>3</sup> and (b) 1.15 g/cm<sup>3</sup>.

with structure II [24]. This clathrate structure is well characterized and can be described as the H-bond network built from ubiquitous pentagonal dodecahedrons (small cages) and 16-hedrons (large cages). In the solid clathrate, the oxygen molecules can occupy both cages. Presumably, some formation of quasi-clathrate cages of H<sub>2</sub>O molecules around hydrophobic O<sub>2</sub> molecules may occur in low-temperature solutions.

Fig. 4 displays (a) the spatial coordination of oxygen molecules around water molecules and (b) the spatial distributions of oxygen atoms of water molecules hydrating a dissolved oxygen molecule are displayed. The simulation results for the SPC/E model of water at temperature 263 K and density 1.0 g/cm<sup>3</sup> containing two oxygen molecules are shown.

Fig. 4. The effect of dissolved oxygen on the spatial structure in low-temperature liquid water. (a) The spatial distributions of oxygen molecules around water molecules and (b) the spatial distributions of oxygen atoms of water molecules hydrating a dissolved oxygen molecule are displayed. The simulation results for the SPC/E model of water at temperature 263 K and density 1.0 g/cm<sup>3</sup> containing two oxygen molecules are shown.

the spatial coordination of water molecules around dissolved oxygen molecules in 0.1 M oxygen–water solution at 263 K. The simulation

results for the simple point charge (SPC/E) [25] model of water are shown; the oxygen molecule is modeled as the Lennard-Jones diatomic containing three imbedded point charges.

The hydration structure forming around dissolved  $O_2$  molecules (Fig. 4(b)) differs radically from that which exists around  $H_2O$  molecules in pure liquid (Fig. (3a)). Water molecules tend to accommodate a hydrophobic particle by forming a distinct hydration shell around it ('donut'). This hydration structure hardly resembles a crystalline cage, yet, on average, it contains around 17 water molecules (which can be found by an integration of the  $O_2$ – $H_2O$  pair-density distributions, see also Ref. [26]) indicative of clathrate forming. Important additional details emerge from Fig. 4(a). It shows that  $O_2$  molecules also tend to align themselves along the direction of OH bonds of water molecules (presumably by forming H-bond type complexes with  $H_2O$ ). Pair-density maxima corresponding to this arrangement are clearly evident in the upper hemisphere of the spatial distribution in Fig. 4(a).

#### 4. Concluding remarks

In this paper we have illustrated with some simple examples (water and dissolved oxygen in water) the analysis of 3D disordered structures arising in molecular liquids. The spatial molecular density maps are now available for many other systems including aqueous nonelectrolyte solutions, nonaqueous H-bonded solvents, nonpolar molecular liquids, etc.; see review [19] and references therein. They result in a detailed understanding of diverse solvation phenomena and help decipher costly experimental neutron scattering and X-ray diffraction data. Further studies in this area may involve the time-dependent SDFs [27], or the local frame resolved pair-density time-correlation functions (the spatial van Hove functions). These pair-density time-correlation functions provide the means not only to portray the local density distributions in complex liquids but also to investigate their fluctuations (dissipations) in any spatial direction.

#### Acknowledgements

We are grateful for the financial support of the Natural Sciences and Engineering Research Council of Canada.

#### References

- [1] P.A. Egelstaff, *Introduction to the Liquid State*, Academic Press, New York, 1967.
- [2] M.P. Allen, D.J. Tildesley, *Computer Simulations of Liquids*, Oxford University Press, Oxford, 1987.
- [3] A.K. Soper, M.G. Phillips, *Chem. Phys.* 107 (1986) 47.
- [4] A.K. Soper, *J. Chem. Phys.* 101 (1994) 6888.
- [5] S.W. Pennycook, *J. Phys. Chem.* 32 (1928) 1681.
- [6] J.D. Bernal, R.N. Fowler, *J. Chem. Phys.* 1 (1933) 515.
- [7] J. Morgan, B.E. Warren, *J. Chem. Phys.* 6 (1938) 666.
- [8] I.M. Svishchev, P.G. Kusalik, J. Wang, R.J. Boyd, *J. Chem. Phys.* 105 (1996) 4742.
- [9] W.L. Jorgensen, J. Chandrasekhar, J.D. Madura, R.W. Impey, M.L. Klein, *J. Chem. Phys.* 79 (1983) 926.
- [10] O.Ya. Samoilov, *Structure of Aqueous Electrolyte Solutions and the Hydration of Ions*, Consultants Bureau, New York, 1965.
- [11] A.H. Narten, M.D. Danford, H.A. Levy, *Dis. Faraday Soc.* 43 (1967) 97.
- [12] J.A. Pople, *Proc. R. Soc. A* 221 (1954) 498.
- [13] M.G. Sceats, M. Stavola, S.A. Rice, *J. Chem. Phys.* 70 (1979) 3927.
- [14] F.H. Stillinger, A. Rahman, *J. Chem. Phys.* 55 (1971) 3336.
- [15] F.H. Stillinger, A. Rahman, *J. Chem. Phys.* 60 (1974) 1545.
- [16] I.M. Svishchev, P.G. Kusalik, *J. Chem. Phys.* 99 (1993) 3049.
- [17] I.M. Svishchev, P.G. Kusalik, *J. Chem. Phys.* 100 (1994) 5165.
- [18] A. Laaksonen, P.G. Kusalik, I.M. Svishchev, *J. Phys. Chem. A* 101 (1997) 5910.
- [19] A. Laaksonen, P.G. Kusalik, I.M. Svishchev, in: P.B. Balbuena, J.M. Seminario (Eds.), *Molecular Dynamics: from Classical to Quantum Methods*, Elsevier, Amsterdam, 1999.
- [20] A.K. Soper, J.L. Finney, *Phys. Rev. Lett.* 71 (1993) 4346.
- [21] D.T. Bowron, A.K. Soper, J.L. Finney, *J. Phys. Chem. B* 102 (1998) 3551.
- [22] P.V. Hobbs, *Ice Physics*, Clarendon Press, Oxford, 1974.
- [23] I.M. Svishchev, P.G. Kusalik, *Chem. Phys. Lett.* 239 (1995) 349.
- [24] J.A. Ripmeester, C.A. Ratcliffe, D.D. Klug, J.S. Tsein, in: E.D. Sloan, M.A. Hnatow (Eds.), *Annals NY Academy of Sciences*, vol. 715, Academy of Sciences, New York, 1994.
- [25] H.J.C. Berendsen, J.R. Grigera, T.P. Straatsma, *J. Phys. Chem.* 91 (1987) 6269.
- [26] E. Fois, A. Gamba, C. Redaelli, *J. Chem. Phys.* 110 (1999) 1025.
- [27] I.M. Svishchev, A.Yu. Zassetsky, *J. Chem. Phys.* 112 (2000) 1367.